Lawrence Berkeley National Laboratory
Recent Work

Title

THE MAGNETIC AND ELECTRICAL PROPERTIES OF SOME METALS AT HIGH PRESSURES

Permalink

https://escholarship.org/uc/item/1dr9x2gm

Author

Phillips, David B.

Publication Date

1965-08-01

University of California

Ernest O. Lawrence Radiation Laboratory

THE MAGNETIC AND ELECTRICAL PROPERTIES OF SOME
METALS AT HIGH PRESSURES

Berkeley, California

DISCLAIMER

UNIVERSITY OF CALIFORNIA

Lawrence Radiation Laboratory
Berkeley, California

AEC Contract No. W-7405-eng-48

THE MAGNETIC AND ELECTRICAL PROPERTIES
OF SOME METALS AT HIGH PRESSURES

David B. Phillips

(Ph.D. Thesis)

August 1965

CONTENTS

THE MAGNETIC AND ELECTRICAL PROPERTIES
OF SOME METALS AT HIGH PRESSURES

David B. Phillips

Inorganic Materials Research Division, Lawrence Radiation Laboratory
Department of Chemistry, University of California
Berkeley, California

August 1965

ABSTRACT

A device for measuring low field magnetization of high permeability
materials as a function of temperature and pressure in Bridgman anvils
has been developed. This device has been used to measure the Curie point
(T_c) of Gd to 20 kbars pressure and the Neel point (T_n) of Tb to 15 kbars
pressure. For Gd dT_c/dP was found to be $-1.9\pm0.2°K/kbar$, and dT_n/dP for
Tb was measured as $-1.4\pm0.2°K/kbar$. The decrease in low field magnetiza-
tion with pressure was quite marked in both cases and this limited the max-
imum pressures obtainable. The decrease in magnetization is shown to be a
result of elastic stresses and plastic deformation caused by compression.
The basic system should be capable of pressures to 100 kbars and a tempera-
ture range of 65-600°K. Suggestions for reaching these conditions and ex-
tending the measurements to higher pressures for Gd and Tb are discussed.

In an attempt to determine the effect of alloying on the high pressure
iron phase transition, the Fe^{57} Mössbauer spectra in two types of stainless
steel were studied at high pressures. No evidence for any sharp phase
transitions was found. In both samples a broad absorption superposed on
the single central line was noted at high pressures. This behavior was
reversible with pressure in one sample and irreversible in the second

- sample. Annealing restored the original spectrum of the second sample. These changes are discussed as a transition from a paramagnetic to a partially ferromagnetic structure under pressure.

The electrical resistance of bismuth has been carefully investigated in the pressure region between 30 and 90 kbars in an attempt to locate the transitions noted as volume discontinuities by Bridgman. No discontinuities were found in the electrical resistance in this region. This does not necessarily mean that the phase changes reported by Bridgman at 45 and 64 kbar do not exist.

MAGNETIC PROPERTIES OF GADOLINIUM
AND TERBIUM AT HIGH PRESSURES

I. INTRODUCTION

Elements with partially filled d or f shells show some unique magnetic properties. As electrons fill the d or f orbitals large atomic magnetic moments are produced. At some temperature the magnetic dipole interaction between adjacent atoms should overcome the thermal energy and the atomic moments should align. The dipole interaction energy for two iron atoms separated by the normal lattice distance is about 1×10^{-16} ergs; Boltzmann's (k) constant is 1.38×10^{-16} ergs/°K; at some temperature near 1°K the thermal energy (kT) will become so small that alignment of atomic moments in Fe metal should occur to produce a large bulk magnetic moment. Actually this orientation is observed in iron metal to a temperature of 1043 °K. An interaction 10^3 times as large as magnetic dipole interaction must be devised to explain this magnetic ordering.

Determination of the radial dependence of the interaction responsible for this magnetic ordering has been of interest both theoretically and experimentally since Heisenberg[1] first proposed a qualitative quantum mechanical basis for this phenomenon. Bethe[2] and others have made crude calculations of the magnitude of a proposed ordering mechanism and have obtained a much reproduced curve showing the strength of this interaction as a function of interatomic distance. The magnetic (order-disorder) transition temperatures must be simply related to the strength of this interaction.[3] Measurement of the volume dependence of the transition temperatures of a series of magnetically ordered, related elements will furnish an empirical interaction-deistance curve with which to compare any calculations.

The phenomenon of parallel alignment of atomic magnetic moments to produce a bulk moment is termed ferromagnetism. The bulk moment of the sample is not always observable in the absence of a magnetic field. It has been shown that the magnetic structure of a macroscopic specimen is broken up into regions (called domains) with the atomic moments aligned parallel in each region but with the net moments of different domains aligned in a manner to lower the bulk moment and, correspondingly, the magnetic energy of the entire specimen.[4]

Another type of magnetic ordering, which would not be expected from any classical interaction, has been shown to exist.[5] Adjacent atomic moments can align antiparallel and in this case no bulk magnetic moment is produced. Such ordering is known as antiferromagnetism.

There are two series of magnetically ordered elements—the (3-d) transition and the (4-f) rare earth metals. Of the 3-d elements, Cr and Mn are antiferromagnetic, and Fe, Ni, and Co are ferromagnetic. The Néel (antiferromagnetic-paramagnetic transition) temperatures of Cr and α-Mn are 311° and 95°K respectively.[6,7] The Curie (ferromagnetic-paramagnetic transition) temperatures of Fe, Ni, and Co are 1043°, 633°, and 1400°K.[8,9] The spin arrangements of ordered Fe, Ni, and Co are simple with all atomic moments in a single domain aligned parallel.[8] Although the crystal structure of α-Mn is quite complex, the ordered spin arrangement, as in Cr, has each atomic moment aligned antiparallel to those of the nearest neighbors.[6,7] In the remaining 3-d and in the 4 and 5-d transition elements no evidence for magnetic ordering has been found.[10-12] More than half of these remaining d-transition elements are superconducting at low temperatures which may preclude any magnetic ordering.[13]

In the 4-f elements Ce, Pr, Nd, Sm, and Eu all show antiferro-magnetic ordering.[14,15] The magnetic properties of Pm, which has no stable isotopes, are unknown. However, it is the last half of the series which is of interest as these elements (Gd, Tb, Dy, Ho, Er, and Tm) all crystallize in a hexagonal close packed structure at the temperatures of interest. Their lattice parameters are very similar, showing a slight decrease with increasing atomic number.[16] Gd has a Curie point at 293 °K; Tb, Dy, Ho, Er, and Tm show more complex behavior with Néel temperatures of 229°, 179°, 132°, 85° and 51 °K and, in addition, ferromagnetic-antiferro-magnetic transitions at temperatures of 221°, 85°, 20°, 20°, and 22 °K respectively.[14] (Whether this ferromagnetic-antiferromagnetic transition should be termed a Curie point is open to some question. These are transitions from one ordered phase to another and usually show a volume change, in contrast to a "real" Curie point. Curie point in quotation marks will be used to denote such a transition.) The spin arrangement in Gd is that of a simple ferromagnet.[17] The antiferromagnetic spin arrangements of the rare earths are complex.[14] The simplest structure consists of atomic moments aligned parallel in the basal plane. The moments in each plane are rotated by some angle with respect to neighboring planes, and the moment vector describes a helix about the c-axis. The period of the turn of the moments is temperature dependent but is of the order of five atomic layers. Such an arrangement of atomic moments results, in a finite crystal, in no bulk magnetic moment. Tb, Dy, Ho, and Er show another important feature. The antiferromagnetic ordering is converted to ferromagnetic in low to moderate applied magnetic fields (about 300 oersteds for Tb). This phenomenon is called weak anti-ferromagnetism.[18,19]

From measurements of the pressure dependence of magnetic transition temperatures and appropriate compressibilities, the volume dependence of magnetic ordering can be derived. The apparatus described in this report is useful for measuring the pressure dependence of Curie points or Néel points of very weak antiferromagnets. The temperature limitations of the system are discussed in the experimental section. Because of their particularly convenient transition temperatures, Gd and Tb were chosen for these initial studies.

The free energy (F) must be continuous across any phase boundary as the free energies of any two phases coexisting in equilibrium are equal. The most familiar type of phase transition is called first order because the derivatives of F, the volume (V) and the entropy (S), are discontinuous at the phase boundary. Using the continuity of F an equation describing the pressure (P) and temperature (T) equilibrium phase line can be derived. This is the familiar Clapeyron equation:

$$\frac{dT}{dP} = \frac{V_2 - V_1}{S_2 - S_1}$$

where 1 and 2 represent the two phases. In a number of important phase transitions the volume and the entropy are continuous across the phase boundary. In this case the Clapeyron equation degenerates to:

$$\frac{dT}{dP} = \frac{0}{0}$$

Assuming that dT/dP does exist, application of l'Hopital's rule (and differentation by T) yields:

$$\frac{dT}{dP} = \frac{\left(\frac{\partial V_2}{\partial T}\right) - \left(\frac{\partial V_1}{\partial T}\right)}{\left(\frac{\partial S_2}{\partial T}\right) - \left(\frac{\partial S_2}{\partial T}\right)}$$

Using the relations:

$$\left(\frac{dS}{dT}\right)_P = \frac{C_p}{T} , \quad \alpha = \frac{1}{V} \left(\frac{\partial V}{\partial T}\right)$$

where C_p is heat capacity at constant pressure and $\Delta\alpha$ is the volume thermal expansion coefficient, it is seen that:

$$\frac{dT}{dP} = \frac{V(\alpha_2 - \alpha_1)}{1/T(C_{p2} - C_{p1})} = \frac{TV\Delta\alpha}{\Delta C_p} . \tag{1}$$

This class of transitions is known as second order because discontinuities arise in the second derivatives of the free energy. The higher temperature magnetic transitions in the heavy rare earths (i.e., the Curie point of Gd and the Neel points of Tb, Dy, HO, Er, and Tm) show no volume or entropy change[20,25-27] and may be considered second order. The heat capacity anomaly (ΔC_p) going from high to low temperature is necessarily positive. Knowledge of the sign of the thermal expansion anomaly then gives the sign of $(dT/dP)_{P=0}$. The thermal expansion anomalies through the magnetic transitions have been measured for Gd, Tb, and Dy and all are negative.[21-23] Good values for $\Delta\alpha$ and ΔC_p could also furnish the magnitude of $(dT/dP)_{P=0}$. Some estimates of these quantities from published reports are given in Table I. It should be emphasized that the magnitudes of these quantities, particularly the thermal expansion anomalies, are approximate. Direct measurement of the transition temperatures as a function of pressure is certainly more accurate and also gives the pressure dependence of dT/dP.

Curie points are defined as the temperature at which the spontaneous magnetization (the magnetization which exists in each domain in the absence of any applied magnetic field) vanishes. At the transition point anomalies arise in many physical properties (e.g. electrical resistivity). Electrical resistance is one of the easiest properties

to study at high pressures, and resistance anomalies have been used to study magnetic transitions as a function of pressure.[29,30]. Such measurements are not always definitive as confusion with a high pressure phase is always possible. The least ambiguous (but not necessarily easiest) method of determining a Curie point at high pressures is measurement of the temperature dependence of magnetization since appearance of a large magnetization is a guarantee of the existence of magnetic ordering. (This reasoning is probably also true for the order-disorder transition point of a weak antiferromagnet). The rest of this report describes an apparatus for making and the results of such measurements.

Table I

	$\Delta\alpha, \frac{1}{^\circ K}$	$\Delta C_p, \frac{cal.}{^\circ K\text{-mole}}$	$V, \frac{cc}{mole}$	$\frac{dT}{dP}, \frac{^\circ K}{kbar}$
Gd	-40×10^{-6} (24)	6.6 (25)	19.88 (28)	-1.02
Tb	-35×10^{-6} (22)	11.1 (26)	19.25 (28)	-0.34
Dy	-60×10^{-6} (22)	8.6 (27)	19.03 (28)	-0.58

Note: one kilobar (kbar) equals 1×10^9 dynes/cm^2

II. EXPERIMENTAL

A. General

High pressures in this laboratory are generated by Bridgman anvils. These are truncated cones four inches in diameter with 1/2 inch diameter faces. The anvils are made with a suitable outer ring (in this case a high strength, low permeability stainless steel called Discalloy) which supports a tungsten carbide rod; the top of the carbide rod serves as the load bearing face (see Fig. 1). Most tungsten carbides are cemented with cobalt metal and have a high magnetic permeability so a special type (Kennametal 601) of binderless carbide was used in this experiment.

The samples used in these experiments were in the form of cylinders (0.370 in. diameter by 0.015 in. high). Both the Gd and Tb were supplied by Research Chemicals, Phoenix, Arizona. Impurities of other rare earth and of transition metals were outside the limits of detection by spectroscopic analysis. The Gd was in rod form; the rod was turned to size and samples were parted off on a lathe. The Tb was in the form of irregular chunks; these were rolled to the proper thickness and samples were punched out.

The samples were contained under pressure by a mineral ring (0.500 in. o.d., 0.375 in. i.d., and 0.018 in. high) of pyrophyllite (approximate composition $Al_2Si_4O_{12}H_2$) coated with fine Fe_2O_3.

Two Bridgman anvils face to face with the sample-containing ring between them forms the high pressure system. The anvils are placed under load in a large hydraulic press. The press construction is simple; a massive iron yoke contains a large piston-cylinder which rests on the inside bottom of the yoke. The space between the top of the piston and the top of the yoke is filled with the Bridgman anvils and spacers.
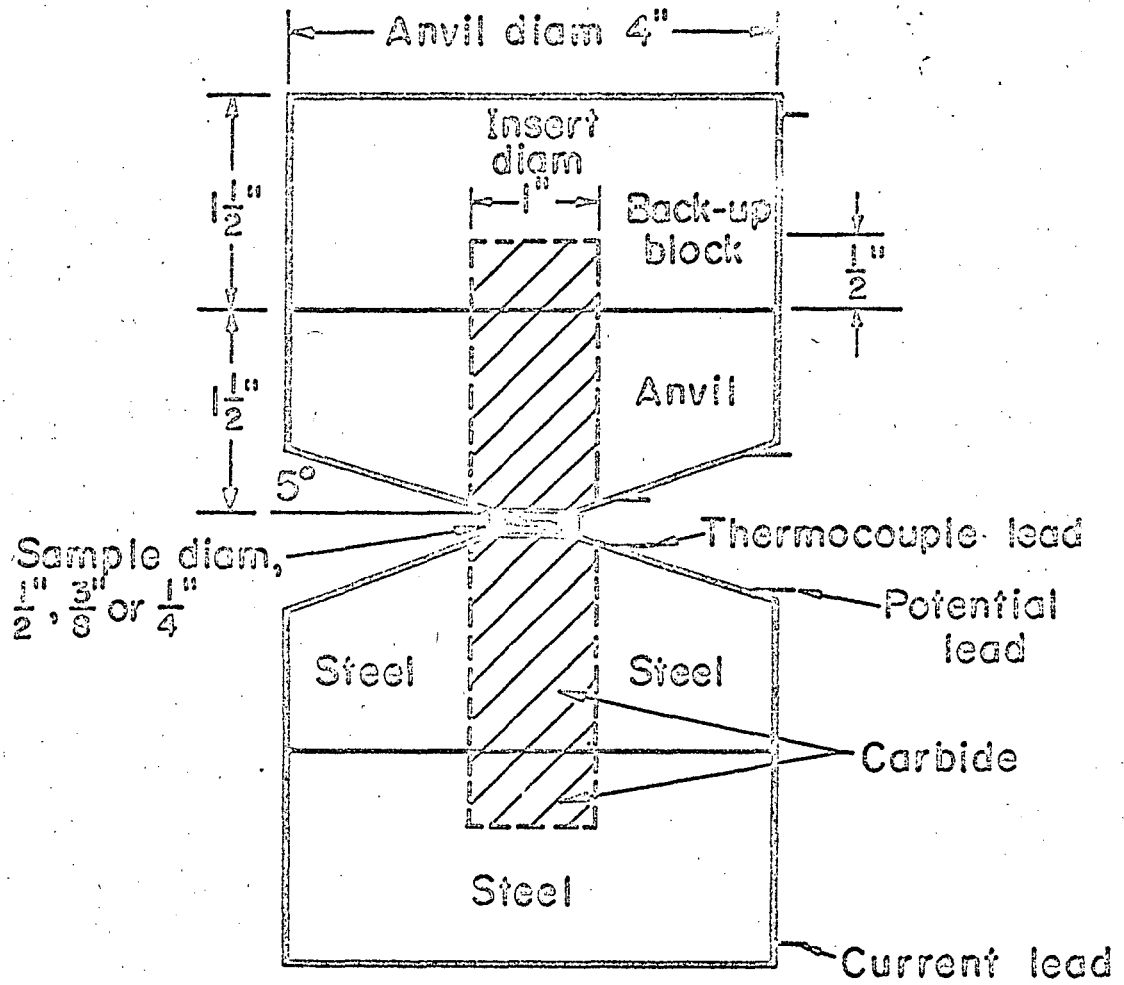
Fig. 1

MU-33473

The force is applied between the top and bottom of the yoke. High pressures are obtained from the large loadings and the small faces of the anvils.

Pressure calibration in this system is a problem. At higher pressures (from about 15 kbars) Bridgman anvil systems can be calibrated by known phase transitions (usually detected by electrical resistance discontinuities). The electrical resistance samples used for calibration are not contained for a reasonable amount of time below 15 kbars. Pressure for these experiments was calculated from the known force and an area corrected for the portion of the containing ring which is load bearing.

Temperature was regulated by placing the anvils and magnetic measuring apparatus in a large, stirred liquid bath. The bath was heated by immersion resistance heaters and was cooled by the flow of a suitable fluid (liquid nitrogen boil-off or methyl alcohol cooled to 195° K in an outside bath) through a heat transfer coil. The resistance heaters were powered by a variable autotransformer and the flow of cooling fluid was controlled by a valve. A temperature change rate of 0.1°K/min could be maintained easily on either heating or cooling in the temperature range 150-320°K. The bath fluid used for the Gd experiments was either toluene (m.p. 178°K and b.p. 383°K) or isopropyl alcohol (m.p. 184°K and b.p. 355°K). The fluid used in the terbium experiments was methyl butane (m.p. 113°K and b.p. 301°K). Because of the low boiling point methyl butane presents serious fire hazards. For safety reasons the entire press was covered with a tight shield. The system was vented to the outside atmosphere and a flow of dry nitrogen gas swept out vapors. This had the dual advantage of reducing fire hazard

and eliminating frost buildup. Water in these bath fluids greatly increases viscosity near the melting point and in polar fluids can cause noise problems from conduction between stirrers, heaters, and the measuring apparatus.

The maximum temperature obtainable (about 350 °K) was limited by the breakdown of the Formvar insulation on magnet wire used to wind the coils described in the next section. Temperatures of 600 °K have been obtained in Bridgman anvils. Modification of the method of heating or use of different insulation on the coil wires could reach such temperatures. The minimum temperature (about 120 °K) is near the lower limit of melting points for bath fluids which boil above room temperature. The heat leak through the anvils and support blocks is very large, and a fluid bath surrounding the anvils helps maintain a uniform, easily controllable temperature at the sample.

An alternative approach is use of·a large quantity of small lead pellets surrounding the anvils to provide a heat sink. By reducing the pressure above liquid nitrogen, temperatures of 65 °K have been reached in large Bridgman anvils. Suitable combinations of these techniques could extend the lower temperature range.

The temperature was measured by copper-constantan thermocouples soldered to the shoulders of the anvils. The voltage of the thermocouples was read from a Keithley 149 milli-microvoltmeter. The actual temperature measured was that of the anvil faces, but, as the whole system was immersed in a large stirred bath and the sample was in intimate contact with the massive anvils, little error was introduced.

B. <u>Magnetic Measurements</u>

A voltage (E) is induced in a coil placed in a changing magnetic field. The voltage is proportional to the time rate of change of the magnetic induction (B), i.e.:

$$E = c \ dB/dt$$

where E is in volts, B in gauss, t in seconds, and c is a constant. The integral of Edt is proportional to the total change in induction in a specified time:

$$B_2 - B_1 = \Delta B = \int_{t_1}^{t_2} c \ Edt$$

Such an integration can be performed electronically using a resistance-capacitance circuit of proper time constant.[31] The magnetic induction is a function of magnetic field strength (H) and the magnetization (M) of the medium:

$$B = H + 4\pi M$$

If two solenoids, one containing a ferromagnetic material, are placed in a large volume, uniform magnetic field in vacuum, any change in the magnetic field strength induces voltages in the solenoids. The difference between the time-integrated voltages of the solenoids is proportional to the magnetization of the ferromagnetic material since the field is assumed to be uniform and the magnetization of the vacuum is zero. These were the guiding principles for the magnetic measurements. Two different devices for making these measurements were built.

The original apparatus, in which some of the measurements on Gd were made, consisted of a pair of electromagnets mounted on the press yoke; the pole tips were 2.5 in. diameter with an air gap of 4.5 in. (see Fig. 2). An iron bar resting on top of the hydraulic piston and fitting closely to the sides of the yoke eliminated the hardened
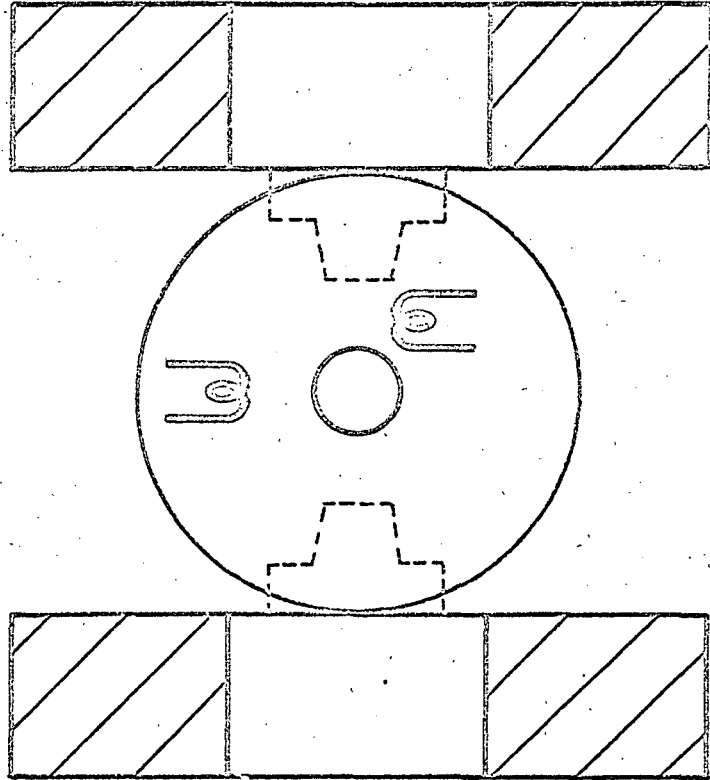
Fig. 2

MU-36535

tool steel piston-cylinder from the magnetic flux path. The field at the center of the gap, with 4 amp current in the electromagnets, was 800 oe uniform to 1% over the volume of the sample. A 300 turn coil, wedge shaped to fit the taper of the anvils, was placed in line with the field about 1/4 in. from the sample to serve as a signal coil; perpendicular to the line of the field and about one inch from the sample was a flat wound bucking coil. The output of the bucking coil was voltage divided and the output of the voltage divider was connected series opposed to the output of the signal coil. The voltage divider was set to give a null integrated signal on field reversal with a para-magnetic sample in place. There are two differences between the ideal magnetization measurement described before and this apparatus. The signal coil does not surround the apparatus but only "samples" the induction at a point some distance away. The surrounding medium in this case is not vacuum but stainless steel and tungsten carbide. For these reasons this apparatus was of marginal sensitivity. Sensitivity was improved slightly by decreasing the air gap and the spatial extent of the magnetic field. This was done by attaching pole tip extensions tapered to fit between the anvil faces. The signal coil was placed between the end of the pole tip and the sample. The evolution of this apparatus indicated a design that would greatly increase sensitivity.

The second apparatus is pictured in Fig. 3. A block figure-eight shaped frame was fashioned of 0.25 in. soft iron. One inch sections were cut from the center of both ends. These ends were tapered to fit between the anvil faces. The frame was then split on the center arm and a 1000 turn field coil was fitted. The frame was rejoined by a strap of soft iron. A 1000 turn signal coil was fitted on either end of
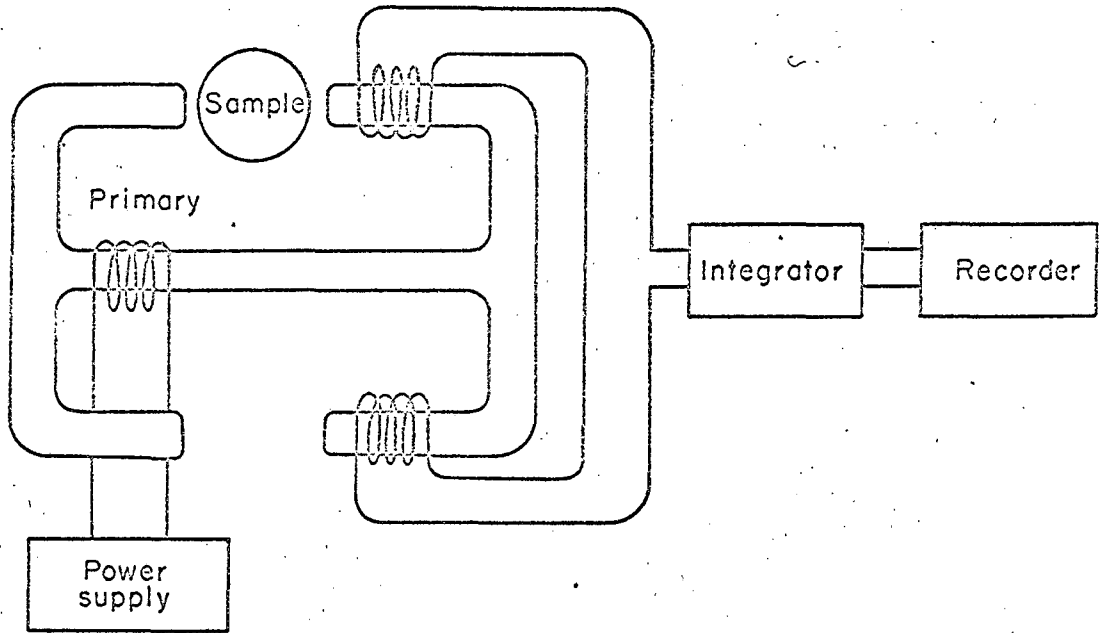
Fig. 3

MUB-5406

the frame. The series opposed output of the two signal coils was balanced (by a voltage divider) to give a null integrated voltage on field reversal with a paramagnetic sample in place. In operation the sample to be studied was placed in one of the gaps; a brass spacer placed in the other gap prevented springing of the arms on field reversal. The field at the center of the gap was about 100 oe with 0.4 amp field coil current.

This apparatus again measures the difference in induction between two points. The induction in this case is largely due to the iron frame. Introduction of a ferromagnetic sample in one of the gaps increases the induction in that portion of the frame and results, on field reversal, in a time integrated voltage difference between the two coils which is proportional to the magnetization of the sample.

Measurements were made at constant pressure as a function of temperature. At each temperature the magnetic field was reversed about 15 times. A few field reversals were necessary to put the iron frame and the sample in a cyclic magnetic state. The last ten field reversals constituted the measurement. The resulting voltage outputs of the integrator were displayed on a Leeds and Northrup recorder. The ten voltage readings were averaged and plotted against temperature. A background curve was obtained by similar measurements on a para-magnetic material. This background curve was subtracted from the read-ings taken on the magnetic specimens to give the final form of the curve.

C. Experimental Errors

The electronic integrator acts as a very high gain voltage amplifier. All solder joints in the input circuit were placed outside the cooled

region to prevent amplification of thermal EMF's. The integrator and its associated circuits have an inherent noise level which is seen as a randomly drifting output. Another form of noise in the circuit is an imbalance in magnetic transients caused by dissimilarities in the two ends of the iron frame. These magnetic transients are seen as oscillations at the end of the voltage change on field reversal. At the gain used for these experiments the uncertainty, introduced by baseline drift and transients, in the integrated voltage signal is estimated to be ±0.2 millivolts. For comparison a 0.370 in. diameter by 0.010 in. high disc of cold-rolled iron gives a signal of about 6 mv.

The temperatures were read to about ±0.2°K from the milli-microvoltmeter.

A Bourdon tube gauge, calibrated by a strain gauge, was used to measure the fluid pressure (acting on the piston) and thus the press load. The estimated uncertainty in load is equivalent to ±0.2 kbar on a 0.5 in. diameter circular surface. The uncertainty in pressure is another matter. There is no reason to suppose that the reproducibility in actual pressure suffers from more than the uncertainty in load. The accuracy, though, may be in error by 10%. This is a systematic error which may be eliminated if a proper calibration is devised.

A magnetized specimen gives rise to a magnetic field (the demag-netizing field) opposite the applied field. To obtain the actual effec-tive field acting on the specimen requires a complex correction or demag-netizing factor dependent on the geometrical shape of the specimen. As the shape of the samples in these experiments changed in an unknown way with pressure, no demagnetizing correction was attempted. Only the re-lative magnetization as a function of temperature was of interest here so

experimental curves contained herein list a "signal" of arbitrary scale

representing the magnetization at an <u>applied</u> field strength of 100 oe.

III. RESULTS AND DISCUSSION .

Curie points are classically determined by isothermal plots of M^2 against H/M (where M is the magnetization and H is the magnetic field strength). The temperature of the isotherm which goes through the origin gives the Curie point. Because of the limited range of field strengths available here and the signal to noise ratio of our circuit, such measurements were not possible. The measurements actually made were of magnetization at a constant field strength ($H_{applied}$ = 100 oe). The Curie point of Gd was first reported as 289°K.[32] The magnetic anomaly in the heat capacity of Gd occurs at 291.8°K.[25] Later measurements have set the Curie point at 293.2°K.[33] Short range order is seen to persist up to 305°K though, and any magnetization measurements made in finite magnetic fields will yield a higher Curie point.[34] The value of 297.4°K at one atmosphere obtained here is not unreasonable in view of the experimental method.

Figure 4 shows a representative series of magnetization-temperature curves (each taken at constant pressure) for Gd. The steepest portions of the curves were extrapolated to zero magnetization to obtain the Curie temperatures. No significant thermal hysteresis was observed at any pressure. The results are gathered in Fig. 5 together with a line T = 297.4°K - 1.9°K/kbar.

The change in Curie point of Gd had been measured before under hydrostatic pressures. The earliest determination was -1.2°K/kbar at pressures to 8 kbar;[35] a later result gave -1.53°K/kbar to 6 kbar.[36] In both cases the variation of the Curie temperature (T_c) was found to be linear with pressure. While this work was being carried out two other reports gave dT_c/dP as -1.60°K/kbar[37] and -1.72°K/kbar.[38] Again

Fig. 4

MU-36467

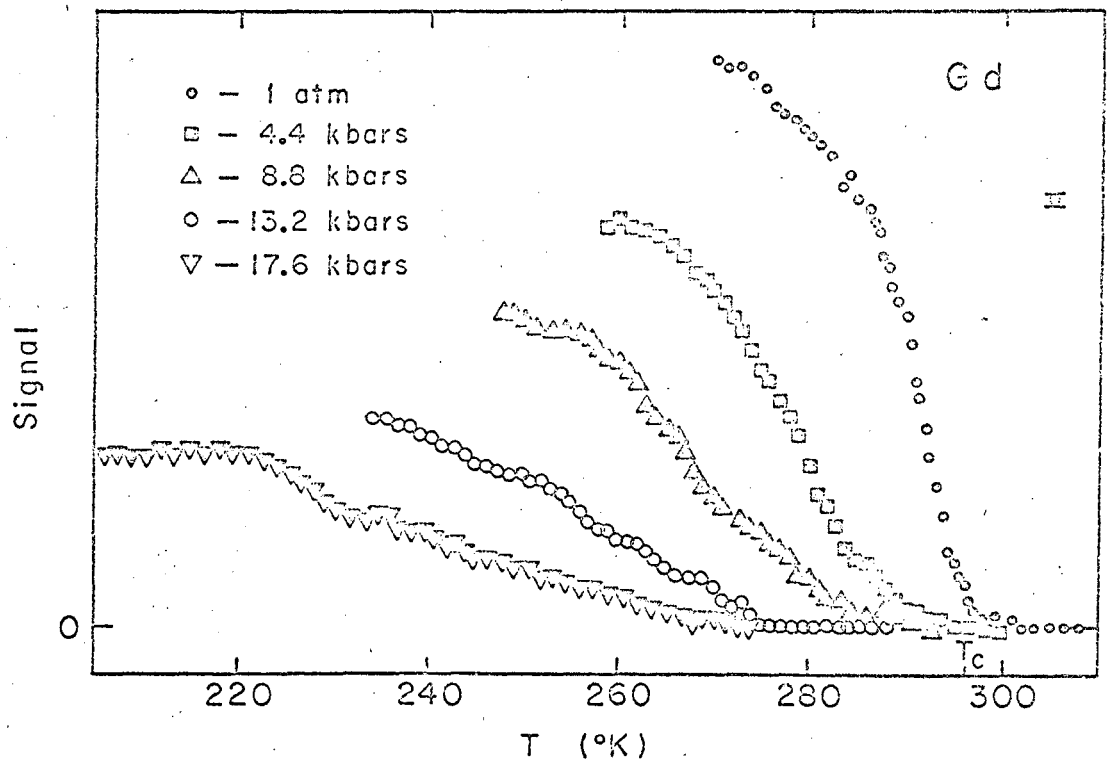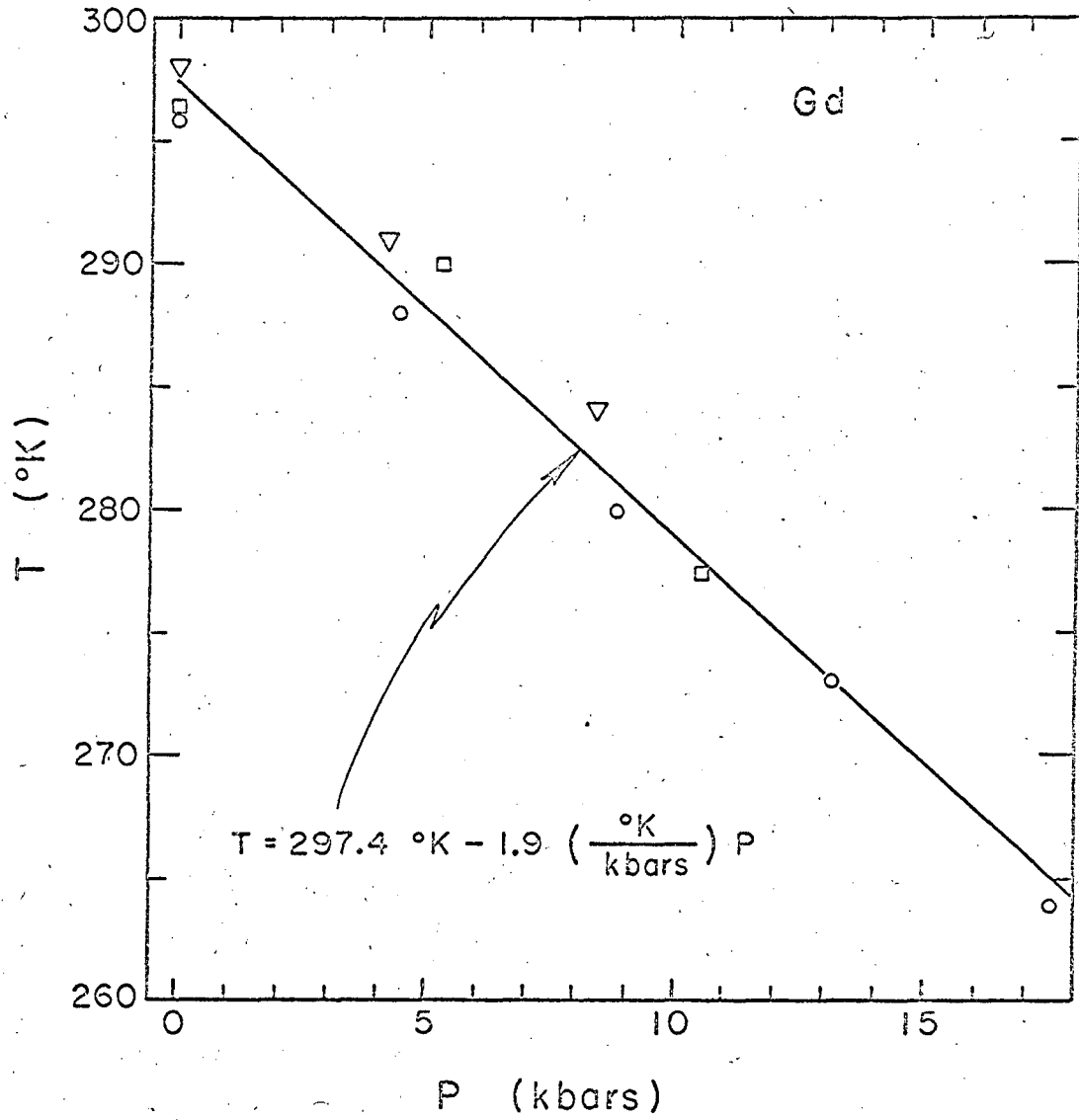$$T = 297.4 \ {}^{\circ}K - 1.9 \left(\frac{{}^{\circ}K}{kbars} \right) P$$

Fig. 5

MU-36471

T_c was a linear function of pressure. The value of dT_c/dP $(-1.9\pm0.2\,°K/$ kbar) obtained here agrees with the later determinations within combined experimental error.

As Fig. 3 shows, the peak signal decreased rapidly with pressure until, at 20-25 kbar, no measurement was possible. This decrease in signal makes determination of the Curie temperature increasingly difficult and also prevents detection of a reported phase change at 25 kbar.[37-39] Two reasons for the decrease in signal can be discussed.

Magnetization at field strengths lower than that necessary to saturate (align all moments in the direction of the field) is dependent on the domain structure of the magnetic material. It has been found in single crystals that the magnetization has certain preferred crystal orientations (the so-called easy directions). On cooling through the Curie point in zero applied field, a ferromagnet expands or contracts along these easy directions. When a magnetic field is applied, the domains oriented favorably with respect to the field grow at the expense of others. At field strengths near saturation, domain growth is not always possible and the magnetization rotates along "hard directions" to line up with the field. The result of all these processes is a change in dimensions of the crystal (but only a slight volume change) as it is magnetized. The phenomenon is known as linear magnetostriction.[40] (Magnetostriction is positive if the material expands in the direction of the field.) Inverse magnetostriction occurs when a ferromagnetic material is elastically stressed. Then, even in the absence of an applied field, the domain magnetizations are oriented (with respect to the stress axis). Table II gives the effect of magnetization at constant field strength (but below saturation) of positive and negative magnetostrictive materials measured parallel or perpendicular to the stress axis.

Table II

Magnetostriction $\left(\frac{1}{l}\right)\left(\frac{\partial l}{\partial H}\right) =$	positive +		negative −	
material under	tension	compression	tension	compression
orientation $H_\parallel$	$M_s > M_u$	$M_s < M_u$	$M_s < M_u$	$M_s > M_u$
$H_\perp$	$M_s < M_u$	$M_s > M_u$	$M_s > M_u$	$M_s < M_u$

Here $\underline{l}$ is the length of the specimen, $\underline{M}$ is the magnetization, and $\underline{s}$ and $\underline{u}$ represent stressed and unstressed material.

In these experiments the compressions are nearly uniaxial (along the axis of the anvils) and the magnetization is measured perpendicular to the stress axis. The magnetostriction of polycrystalline Gd is a complex function of temperature. It is negative at low temperatures and goes to zero in the vicinity of the Curie point.[41] The effect of the elastic compressive stress and the negative magnetostriction is to lower the magnetization at a given field strength. This limitation cannot be overcome until a much more sophisticated system, capable of measuring saturation and spontaneous magnetization under pressure, can be built.

The second effect causing a decrease in signal is that of plastic deformation brought about by the pressure gradient which exists in Bridgman anvils.[42] As described briefly earlier, the process of magnetization of a macroscopic specimen involves first the growth of domains oriented favorably with respect to an applied field and secondly the rotation toward the field direction of the magnetization within other domains. The magnetization rotation requires considerably more energy than does domain growth if the anisotropy responsible for easy and hard directions

of magnetization is significant.[40] In Gd this anisotropy is large and there is only one easy direction (the c-axis). If domain growth is somehow limited in Gd, much higher fields will be necessary to reach saturation magnetization. In polycrystalline Gd the grain boundaries limit domain growth and saturation can be reached only by magnetization rotation in those grains whose c-axis does not coincide with the applied field. In this experiment polycrystalline specimens are the starting material so the effect of the initial grain boundaries is always present. However, any plastic flow induced by the pressure gradient would introduce areas of material which, while not necessarily forming new grain boundaries, might well act as barriers to magnetic domain growth because of the loss of normal lattice periodicity. The result is a decrease in the bulk magnetization at constant, low field strengths. Some progress has been made in annealing samples under pressure by heating for a short time with large current pulses.[43] Such annealing might minimize the effect of plastic deformation on magnetization.

No quantitative separation of these two effects was attempted. From comparison of annealed and cold-worked samples it is estimated that plastic deformation and elastic stresses may contribute about equally to the decrease in signal in Gd.

A final experimental note on Gd should be added here. The volume magnetostriction (change in volume on magnetization) is not zero. After saturation magnetization is reached, and changes in dimensions due to domain alignment are no longer possible, the volume of ferromagnetic material is found to depend on the applied magnetic field. The fractional volume change is linear with field strength. The volume magnetostriction has been measured for both polycrystalline[41,44] and single crystal

Gd.[44,45] The volume magnetostriction is related, on the assumption that the magnetization (M) is a function of T/T_c, by thermodynamics to the change of Curie point (T_c) with pressure (P):

$$\frac{1}{T_c}\frac{dT_c}{dP} = \frac{\left(\frac{\partial\omega}{\partial H}\right)}{T\left(\frac{\partial M}{\partial T}\right) - 3\left(\frac{\alpha T}{\kappa}\right)\left(\frac{\partial\omega}{\partial H}\right)} \tag{2}$$

Where $\omega = \frac{\delta V}{V}$, the fractional volume change, and the other symbols have the meaning used throughout.[46] This equation does not depend explicitly on the Curie point being thermodynamically second order. These quantities are evaluated in Ref. 45, and dT_c/dP is calculated to be -1.26 k/kbar. This gives another indication that both sign and magnitude are nearly correct.

The magnetic properties of terbium were apparently first investigated in 1937.[47] The sample must have been very impure as no magnetic ordering was observed at temperatures well below 200°K. The first measurements on magnetically ordered Tb were made in relatively high fields (about 15,000 oe). Tb was reported to be ferromagnetic with a Curie temperature of 230°K.[48] Later magnetic studies showed a Néel point of 230°K and a ferromagnetic-antiferromagnetic transition at 218°K.[18] Recent magnetic and resistivity,[49] x-ray diffraction,[20] and neutron diffraction[50] studies on Tb single crystals fix the Néel point at 229°K and the "Curie point" at 221°K. Heat capacity anomalies were observed at 227.7°K and 221°K.[27]

Terbium, as noted before, is a weak antiferromagnet between 221° and 229°K.[49] Measurements on polycrystalline samples made in fields of 50-150 oe show a rapid drop in magnetization as the temperature is raised to about 220°K. The magnetization then rises to a peak at 229°K and drops off rapidly above that temperature. In fields of 800 oe and

higher the magnetization curve appears to be that of a normal ferro-
magnet with a Curie temperature of 230°K.[18]   This behavior arises from
alignment of the helical spin structure[14] into the structure of a
ferromagnet.

Figure 6 illustrates the behavior of Tb in this experimental
apparatus with a field strength of 100 oe. As the temperature approaches
220°K the signal drops rapidly, much as in Gd. The signal then rises to
a peak at 228°K and drops to zero above. Extrapolation of the lower
temperature portion of the curve yields a "Curie point" of 224°K. The
Néel point is taken as 228°K, the position of the peak maximum. Figure 5
also illustrates the pressure dependence of the magnetization. In the
curves taken at 5 and 10 kbar a maximum, after a slow drop, in a signal
is seen. Assigning the Néel points (T_n) to the positions of the peak
maxima yields:

$$dT_n/dP = -1.4 \pm 0.2 °K/kbar.$$

After this work was carried out, two reports of the change in Néel
point of Tb with pressure were published. Low field (about 1 oe)
magnetization measurements gave dT_n/dP as $-1.07°K/kbar$[38] in good agree-
ment with this work. A series of compression measurements at various
temperatures showed dT_n/dP to be $0.7°K/kbar$.[51] This is particularly
disturbing as even the sign of the effect is opposite to that obtained
here. From thermal expansion and heat capacity anomalies, Eq. 1
predicts that dT_n/dP will be negative. It can always be argued that the
transition is not strictly second order, even though no volume change
at the transition point has been measured, and so Eq. 1 is not applicable.
Equation 2, however, is based on different assumptions. Magnetostriction
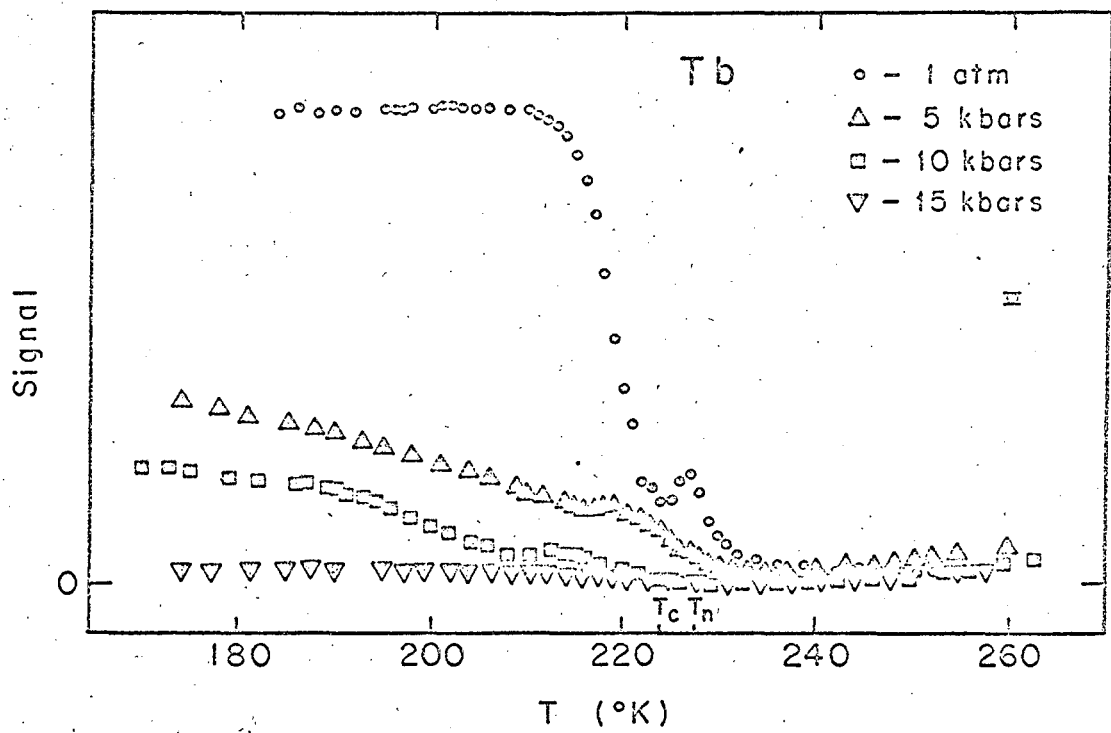in weak antiferromagnets is similar to that in ferromagnets. The volume

Fig. 6

MU-36468

magnetostriction of Tb has recently been measured.[52] Although all the

quantities in Eq. (2) have not been evaluated, the volume magnetostriction

at the Néel point is found to be positive. One of the relations used

in deriving Eq. 2 is:[46]

$$\left(\frac{\partial \omega}{\partial H}\right)_P = -\frac{1}{M}\left(\frac{\partial M}{\partial P}\right)_H$$

A positive volume magnetostriction then predicts a decrease in magnetiza-

tion (at constant field strength) with increasing pressure. Strong

arguments can be given that this decrease in magnetization is caused by

a decrease in transition temperature. Both Eqs. 1 and 2 seem to predict

a negative dT_n/dP and cast some doubt on the positive value.

The decrease in signal with pressure for Tb is quite marked with

meaningful signals disappearing between 10 and 15 kbars. No "Curie

point" could be obtained from the higher pressure curves. Figure 7

shows the drastic effect of plastic deformation on the magnetic properties

of Tb. The magnetization curve of an annealed sample at one atmosphere

is compared to magnetization curves for samples compressed to 5, 10, and

15 kbars and then decompressed to one atmosphere. Annealing the com-

pressed samples for 15 minutes at 1200°K restored the original behavior.

Discussion of the effects of plastic deformation on Tb is complicated by

the fact that it is a weak antiferromagnet and not a ferromagnet. Apparent-

ly the antiferromagnetic ordering is made even weaker by these defor-

mations although the presence of a maximum or a change in slope in each

curve at 228°K indicates the retention of some antiferromagnetism in the

compressed samples. The effects of linear magnetostriction and elastic

stresses on the antiferromagnetic ordering are not well known and are

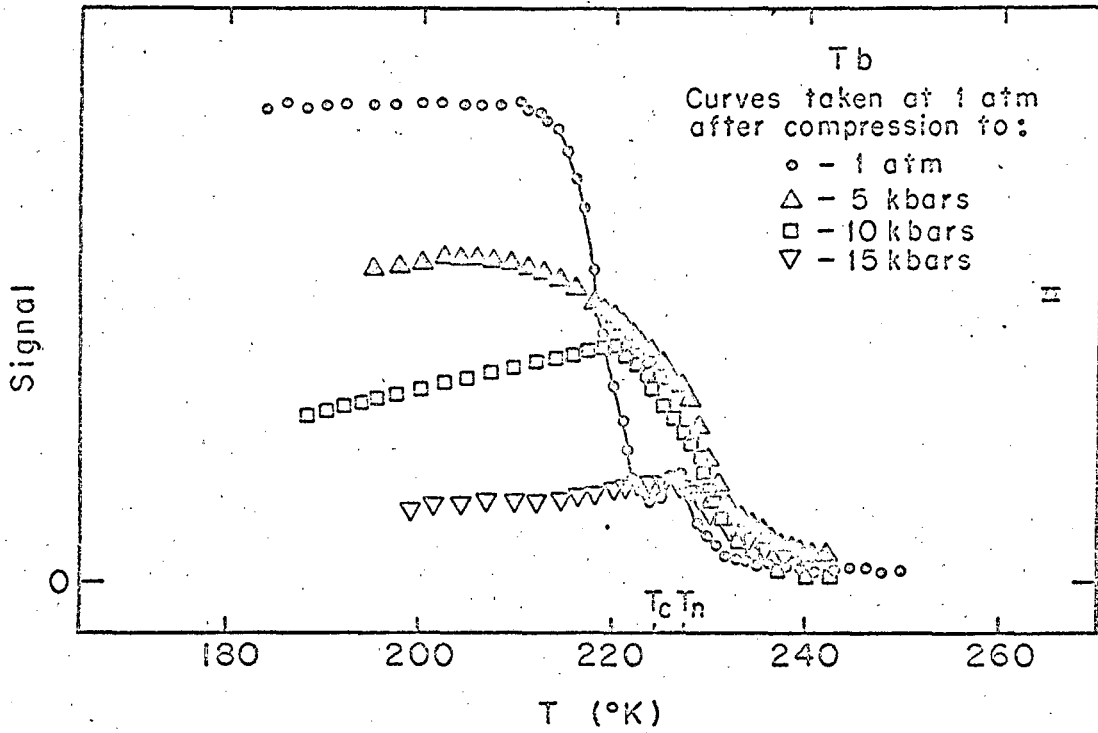obviously outweighed by the effects of plastic deformation. Measurement

Fig. 7

MU-36469

of dT_c/dP and extension of the measurements of dT_n/dP for Tb must await

further development of the technique for annealing under pressure.

In early quantum mechanical calculations on the hydrogen molecule

it was found that the total energy had a component called exchange

energy (E_x) which was dependent on the relative orientations of the

spins of electrons in the molecule. The exchange energy for a two

electron molecule is often written as:

$$E_x = -J (\vec{S}_1 \cdot \vec{S}_2 + 1)$$

where S_1 and S_2 are the spins of the two electrons and J is known

as the exchange integral. For a positive J parallel spin orientation

(triplet state) corresponds to minimum total energy. It was proposed

that this simple treatment could be extended to solids, and that with

iron group atoms in a solid direct exchange interaction would lead to

a positive J and parallel alignment of electron spins as the ground

state of the entire crystal.[1] This was the earliest quantum mechanical

explanation of ferromagnetism. The possibility of direct exchange

interaction in solids yielding a negative J and antiparallel alignment

of electron spins seems to have been neglected, although by analogy

this would lead to antiferromagnetic ordering. Recent calculations

on iron group solids using appropriate wave functions yield exchange

integrals much too small in magnitude and of the wrong sign to explain

ferromagnetism in Fe, Ni, and Co.[53] Direct exchange interactions can at

best give only a qualitative understanding of the mechanisms of magnetic

ordering.

The need for other explanations of magnetic ordering was made very

plain when compounds such as MnO were found to be antiferromagnetic.

Any direct exchange interaction between Mn^{+2} ions would be of very small

magnitude as the Mn^{+2} ions are separated by normally diamagnetic O^{-2} ions. An interaction which involves polarization of the O^{-2} ions to maintain a particular spin alignment between Mn^{+2} ions has been proposed;[54] this theory is adequate to explain the antiferromagnetism of MnO.

Interatomic exchange interactions between the tightly bound 4-f electrons in rare earth metals are certainly very small.[55] The mechanisms proposed for alignment of atomic 4-f electron spins in rare earth metals usually involve interactions between these electrons and the conduction electrons;[56] the latter are not localized but extend throughout a crystal, and may be capable of carrying long range interactions. The exchange interaction in these proposed mechanisms is between the rare earth ion core and the conduction electrons. The 4-f electronic structure and the atomic magnetic moment of the rare earth metals are considered to be volume independent for moderate compression. With these approximations the volume dependence of the energy of magnetic ordering and correspondingly the volume dependence of the magnetic transition temperatures can be written as:[57]

$$\frac{d\ln T}{d\ln V} = \frac{d\ln N(^\epsilon F)}{d\ln V} + \frac{d\ln|I|^2}{d\ln V}$$

where $N(^\epsilon F)$ is the density of states at the Fermi surface for the conduction electrons and I is the strength of the exchange interaction between the ion core and the conduction electrons. From the measurements of dT_c/dP for Gd and dTn/dP for Tb and compressibility measurements, the quantity $\frac{d\ln T}{d\ln P}$ can be calculated. Table III gives these quantities for Gd and Tb and also for Dy and Ho from other reports.

TABLE III

	Gd	Tb	Dy	Ho
$\dfrac{dT}{dP}$ (°K/kbar)	-1.9	-1.4	-0.66 (38) -0.62 (29)	-0.48 (38)
$\dfrac{1}{V}\dfrac{dV}{dP}$ (kbar)$^{-1}$	-2.3×10^{-3} (58)	-2.5×10^{-3} (51)	-2.6×10^{-3} (59)	-2.6×10^{-3} (59)
$\dfrac{d\ln T}{d\ln V}$	2.9	2.4	1.4 (38) 1.3 (29)	1.4

Here T represents the Curie temperature of Gd and the Neel temperatures of Tb, Dy, and Ho.

The quantity $\dfrac{d\ln N(\epsilon_F)}{d\ln V}$ can be derived from careful measurements at low temperatures of specific heat in a magnetic field and of thermal expansion coefficients.[57] Both $\dfrac{d\ln N(\epsilon_F)}{d\ln V}$ and $\dfrac{d\ln I}{d\ln V}$ could be derived from electron paramagnetic resonance measurements as a function of pressure.[57] If these measurements are made, comparison of derived and experimental values for $\dfrac{d\ln T}{d\ln V}$ will provide a good test of these theories.

MÖSSBAUER SPECTRUM OF Fe^{57}
IN STAINLESS STEEL AT HIGH PRESSURES

I. INTRODUCTION

Recoilless emission and absorption of gamma rays (the Mössbauer effect) has proved to be a valuable tool for atomic scale solid state studies.[60] Recent Mössbauer measurements at high pressures are an indication of its value in this area.[61,62] The first Mössbauer effect reported at high pressures was of Fe^{57} in iron metal.[62] A high pressure phase of iron has been known to exist for some time.[63] The Mössbauer experiment showed the phase transition by the collapse of the normal hyperfine splitting into a single line. To study the effect of alloying on the iron high pressure phase transition, it was desired to observe the Mössbauer effect at high pressures in stainless steels.

II. EXPERIMENTAL

Two commercial stainless steels (hereinafter called SS), numbers 304 and 310, were machined into rings 0.184 in. outside diameter, 0.162 in. inside diameter, and 0.007 in. high. The SS 304 was analyzed and found to contain 70.3% Fe, 18.8% Cr, 9.0% Ni, and 0.8% Mn; the SS 310 on analysis showed 53.3% Fe, 23.2% Cr, 19.7% Ni, and 1.8% Mn. The remainders were presumably largely Si with some C, P, and S present. The SS rings were electroplated with Co^{57} on one third of the surface and heated at 1200°K for several hours to diffuse the radioactive material into the body of the steel. Aluminum discs 0.160 in. diameter were placed inside these rings to fill the remaining volume in the pressure cell. This assembly was placed within a pyrophylite ring with

the dimensions 0.250 in. outside diameter, 0.187 in. inside diameter, and 0.010 in. high. The pressures were generated in 0.250 in. diameter face Bridgman anvils.

The Mössbauer spectrometer has been described in detail before[64] and will only be reviewed briefly here. The Co^{57} decays by electron capture to the 137-keV state of Fe^{57}; the excited state Fe^{57} can decay directly to the ground state or can decay by emission of 123-keV and then 14.4 keV gamma rays. The 14.4-keV state is the Mössbauer nucleus and 91% of the Co^{57} decays through this state.[65] The 14.4-keV radiation is detected by a NaI(Tl) scintillation crystal mounted on the face of a phototube. The radioactive source, being under pressure, was held stationary while the absorber (a 0.007 in. thick stainless steel foil enriched to 91% ground state Fe^{57}) was moved to provide a Doppler velocity to trace out the resonance line. Square pulses representing detected 14.4-keV radiation are amplitude modulated with the sine wave velocity of the absorber. The amplitude of a square pulse is proportional to the velocity of the absorber at the moment of detection of the radiation. The series of modulated pulses is fed to a multichannel analyzer for accumulation and storage. The contents of the analyzer were punched onto paper tape and data reduction was done on the Chemistry Department's SDS 920 computer. As the velocity of the absorber is not a perfect sine wave, normalization of the spectra by an experimental curve is necessary. The experimental normalization is obtained by placing the detector so that no resonant absorption is possible. The velocity sweep covered 350 channels on the 400 channel analyzer; the velocity sweep was large enough so that the spectra covered only about 300 channels. The velocity scale was calibrated with the Mössbauer spectraum of Fe^{57} in iron metal. The hyperfine splitting of this spectrum is known accurately.[65]

The fraction of recoilless events should increase with pressure as the Debye temperature of the solid increases. The increase is not measurable in this system as the 14.4-keV radiation is severely attenuated by the containing ring but the higher energy radiation is not. The counting system does not have perfect resolution but counts high energy radiation incompletely absorbed by the detector and scattered high energy radiation as 14.4-keV. The ratio of 14.4-keV to higher energy radiation appearing outside the anvils decreases with increasing pressure and so does the apparent recoil free fraction.

III. RESULTS AND DISCUSSION

The initial spectra of both SS 304 and SS 310 samples were similar and consisted of a single broad line centered at zero velocity with respect to the stainless steel absorber. Figure 8 shows the spectrum of SS 304 at 1 atmosphere pressure and 300°K with the sample placed outside the anvils. Figure 9a shows the same spectrum with the sample placed in the anvils. The Mössbauer spectrum of SS 304 at a pressure of 60 kbars in shown in Fig.11. The central line is still present but a broad absorption extending over a velocity range of about 10 mm/sec is to be noted. All spectra above 40 kbars for both SS 304 and SS 310 showed the same features. Spectra were taken to pressures of 130 kbars for SS 304 and 150 kbars for SS 310. At these pressures the apparent recoil free fraction was less than the statistical error (0.5%). The main difference between SS 304 and SS 310 was to be seen on decompression. Figures 9b and 10 show the Mössbauer spectrum of SS 304 at 1 atmosphere pressure after compression to 130 kbars. The spectrum shown in Fig. 10 is taken with the sample outside the anvils and clearly shows the broad absorption superposed on the central line. Annealing for several hours at 1200°K restored the original single line spectrum of the SS 304. At 1 atmosphere pressure after compression to 150 kbars the SS 310 spectrum was unchanged from the spectrum before compression.

In summary, none of these results show any indication of a sharp phase change in the stainless steels. The broad absorption is attributed to a change from a paramagnetic state to a partially ferromagnetic state. There seem to be several types of sites which display the hyperfine splitting and this prevents resolution of the splittings. The "phase change" in SS 310 is apparently reversible with pressure but

the "phase change" in SS 304 is irreversible; the latter material must be heated to restore the original paramagnetic state.
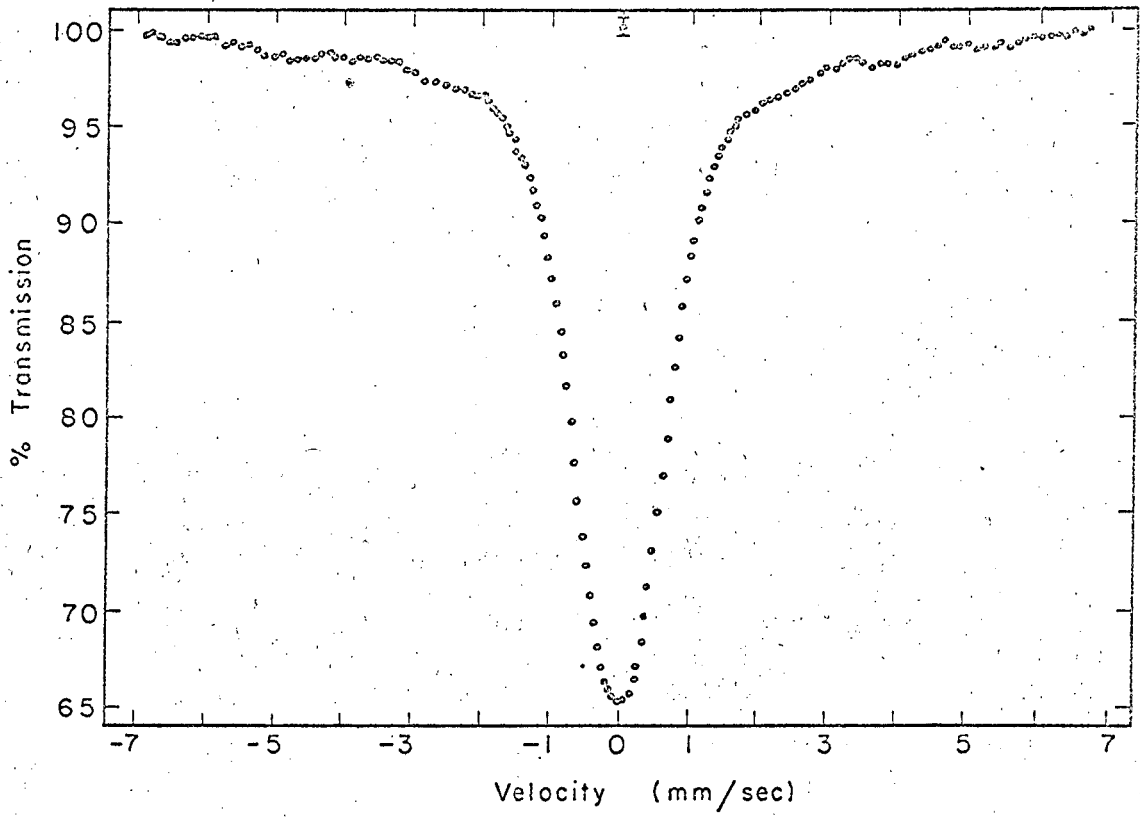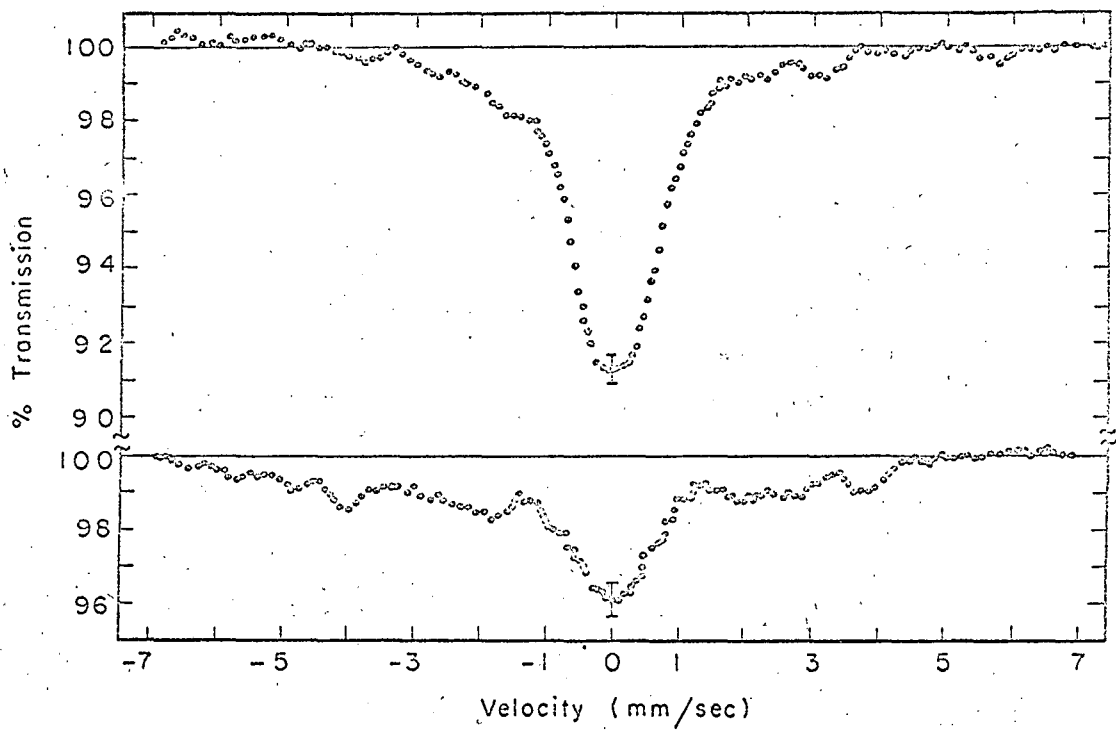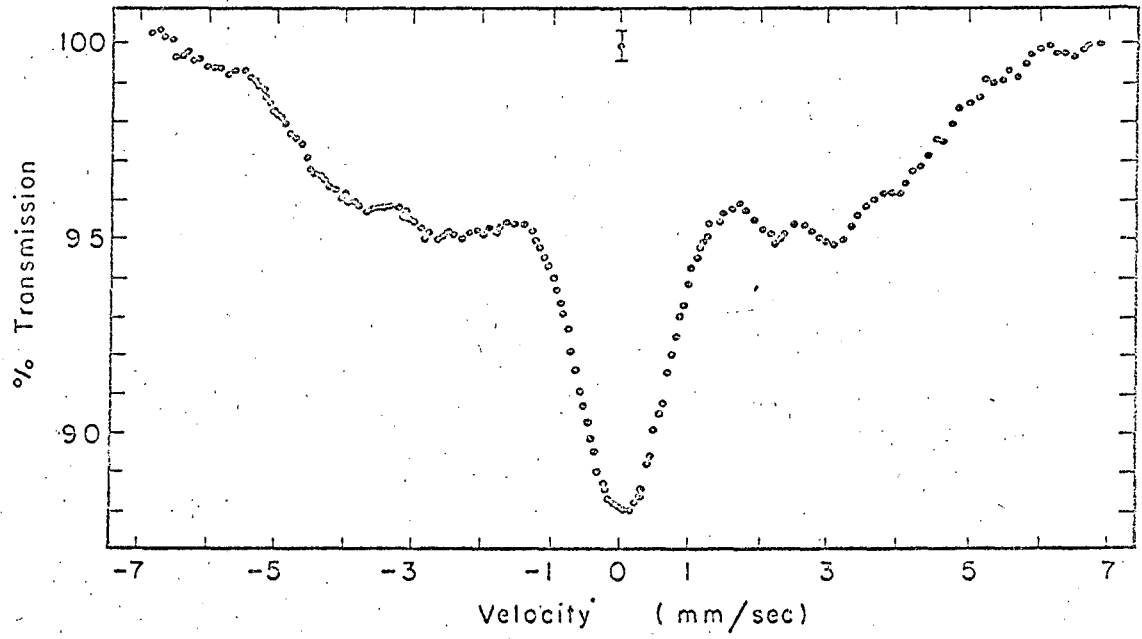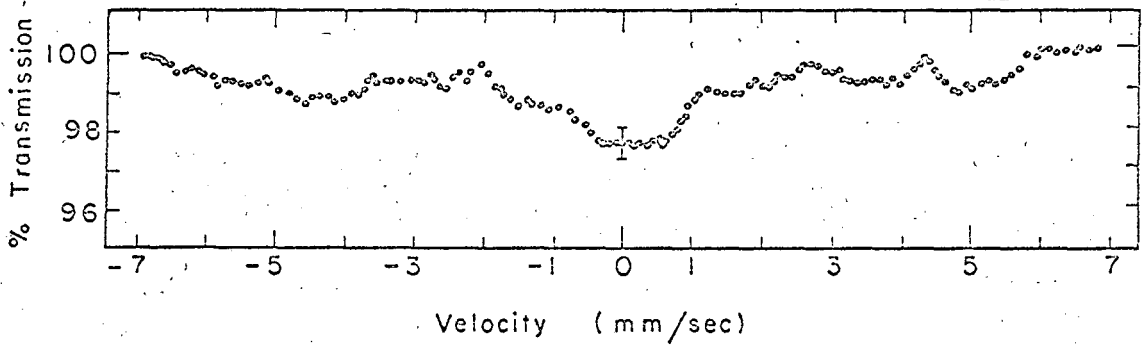
Fig. 8

MU-36531

Fig. 9

MU-36532

Fig. 10

MU.36530

Fig. 11.

MU.36533

THE ELECTRICAL RESISTANCE
OF BISMUTH FROM 25 TO 80 KILOBARS

I. INTRODUCTION

When Bridgman determined the volume-pressure relationships of bismuth to 100 kbar, he found two small volume discontinuities at 45 and 64 kbar.[67] Probably every investigator in high pressures has determined the electrical resistivity of bismuth in this pressure range. Until Zeitlin and Brayman[68] reported discontinuities in the resistance of bismuth at these pressures, no one had found resistance discontinuities that corresponded to the volume discontinuities at 45 and 64 kbars. Because of this report, a more careful determination of the resistance of bismuth as a function of pressure was undertaken. The results indicate that there is no discontinuity in the resistance that is greater than 0.1%. This is much smaller than the discontinuity reported by Zeitlin and Brayman.

II. EXPERIMENTAL

Electrical resistance samples for Bridgman anvils are constructed as shown in Fig. 12. Bismuth wire, 0.003 in. diameter, is bent into a circle and placed concentrically between two 0.370 in. diameter by 0.0035 in. high AgCl discs. Placing a circular sample concentric with the anvil faces minimizes the effect of the radial pressure gradient which exists in Bridgman anvils.[42] Gold plugs 0.020 in. diameter and 0.005 in. high are inserted in the AgCl discs to provide electrical contact between the anvil faces and the sample. The sample is placed in a pyrophyllite ring (0.500 in. outside diameter, 0.375 in. inside diameter, and 0.010 in. high) and the whole assembly is placed between
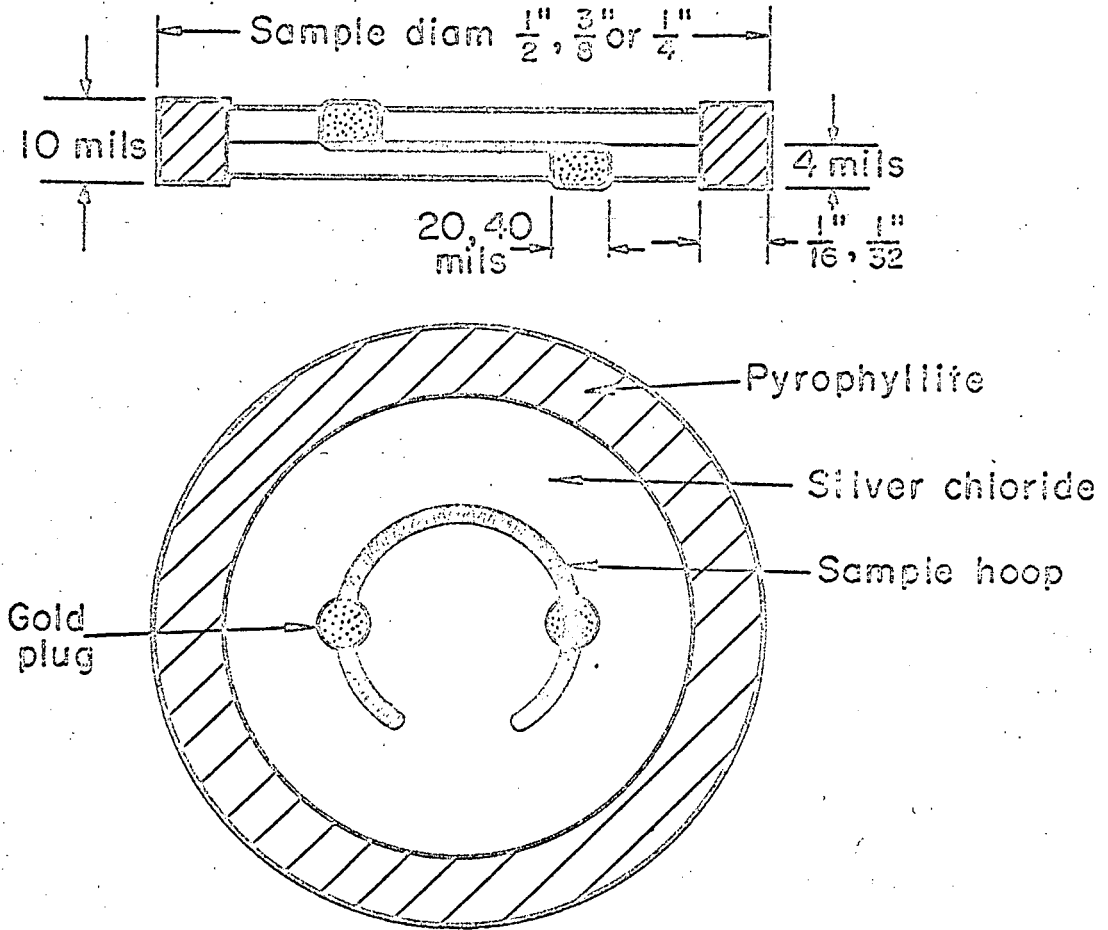
Fig. 12

MU-33474

0.500 in. diameter face Bridgman anvils. Electrical resistance is
usually determined by passing a constant current through the anvils
(as shown in Fig. 1) and measuring the potential drop across the
anvil faces. In this experiment, resistance was measured across the
anvils by a Leeds and Northrup Mueller bridge. The measured resistance
included resistance of the leads and anvils and contact resistances as
well as the sample resistance. The resistance of the leads and anvils
was less than 1% of the total resistance.

The room was air conditioned, and the maximum variation in room
temperature (about 3°C) was so small that it was not necessary to
consider the resistance change in the bridge leads. The anvils were
kept in an oil bath which was thermostated to 301°±0.1°K. The press
has a large diameter ram and low pressure oil system. A strain gauge
in conjunction with a Baldwin-Lima-Hamilton SR-4 bridge was used for
the determination of the load. The sensitivity of the load measure-
ment was 25 bars. The stability of the press is such that in a period
of 12 hours the load would decrease by no more than 0.5%. During the
day, the load was monitored and kept within 0.1% of the assigned value.

III. RESULTS AND DISCUSSION

The resistance of the sample (see Fig.13) through phase II and in
phase "VIII" were determined in the usual fashion, about two minutes
after each pressure increment. In the intermediate region, the region
of interest, the sample was permitted to stand until a resistance
reading was obtained that was constant in the fourth decimal, a part
in 20,000. This took several hours after a compression of 2 kbars.
The resistance came to 0.2% in about two minutes and then drifted down-
ward at a very slow rate for two or three hours afterwards. When all

factors are considered, the relative accuracy of the various resistances in a given experiment should be less than 0.1%.

Three complete experiments were performed. In each case the behavior before and after the region of interest agreed closely with our previous work and that of other investigators. We found no indication of a resistance discontinuity in the 40 or 60 kbar region. We can only conclude that Zeitlin and Brayman obtained spurious results for some reason that we are not in a position to determine.

We found that the most satisfactory method of showing our results was to fit a least squares quadratic expression to our data, and then show the deviation from this fit. This is shown in Fig. 1. This representation is purely empirical and is not meant to imply that this is the correct representation of the resistance of bismuth as a function of pressure. The average deviation of a single and all three determinations is 0.06%, a figure that is reasonable with our expected error. What is more important, there appears to be no systematic deviation.

The lack of discontinuity in the resistance cannot be taken as absolute proof that the phases reported by Bridgman do not exist. There are systems which do not exhibit a discontinuity in the resistance accompanying a phase change. Lanthanum is such a case.[5]
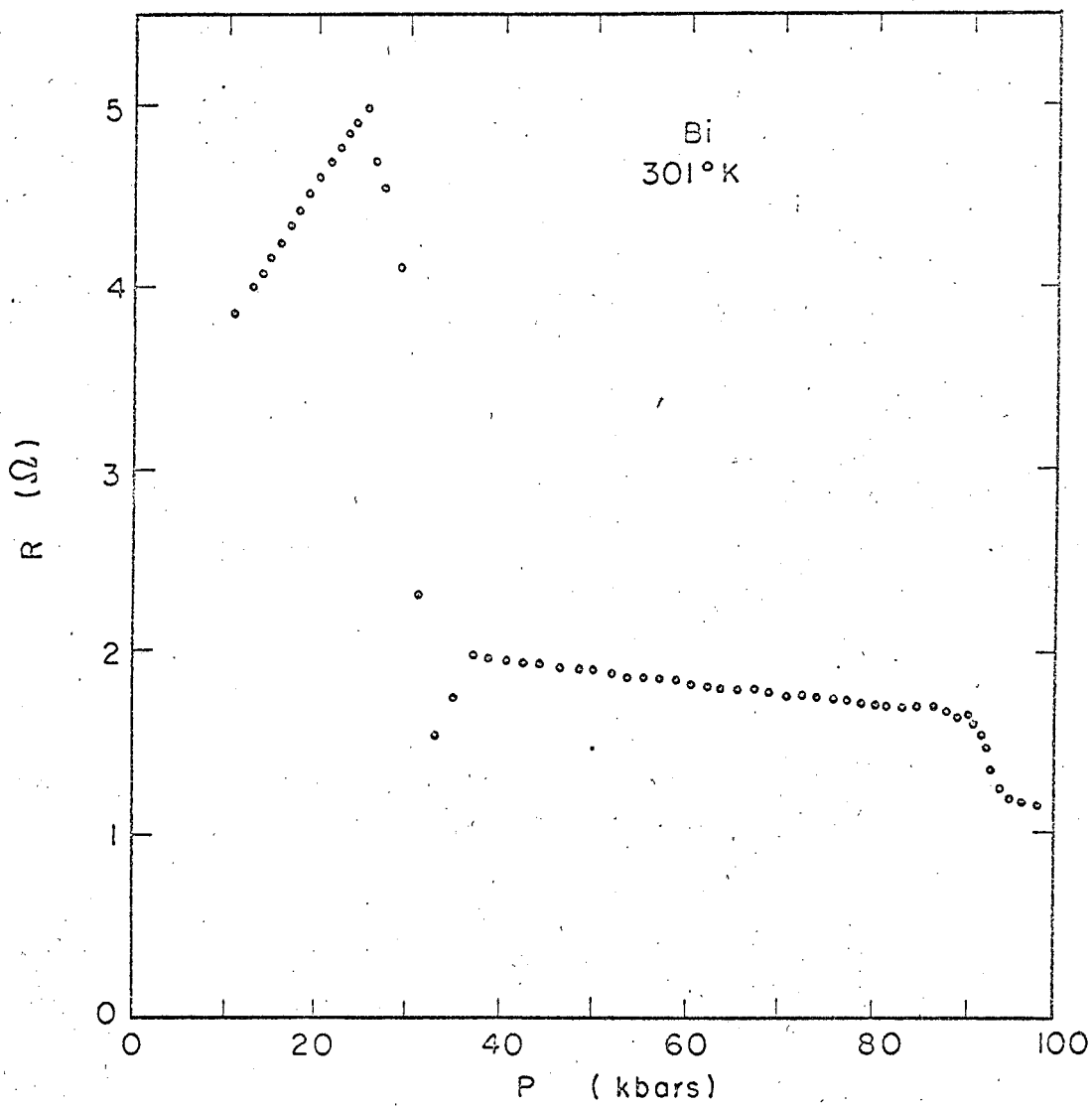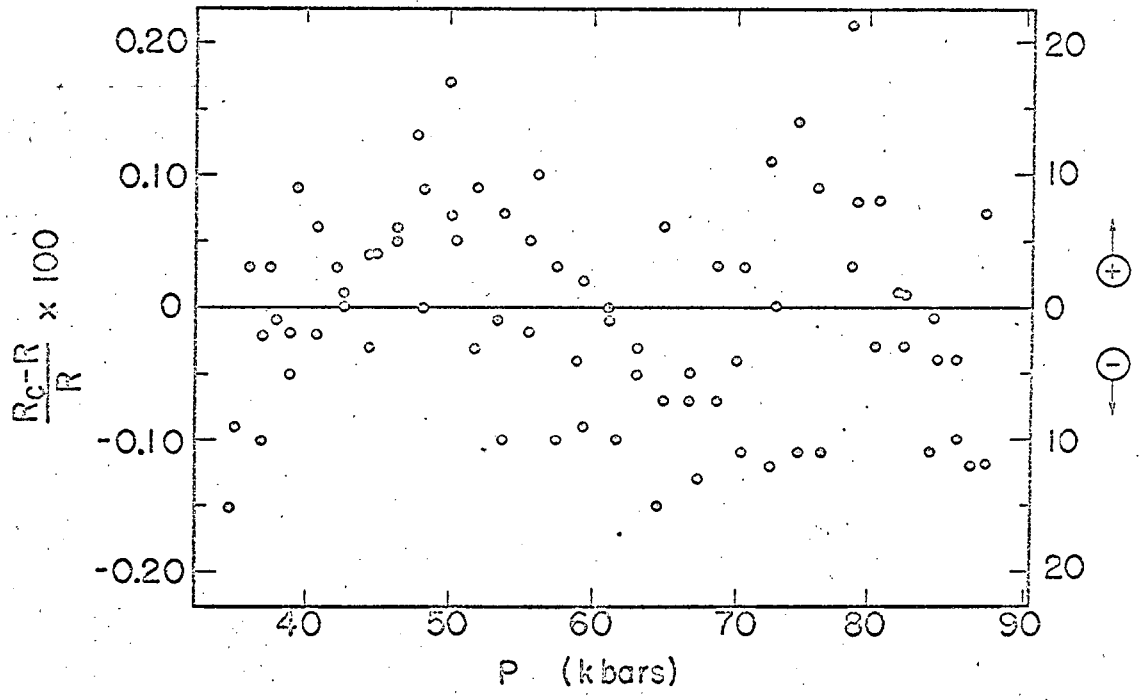
Fig. 13

MU-36534

Fig. 14

MUB-4109

ACKNOWLEDGMENTS

REFERENCES

1. W. Heisenberg, A. Physik 49, 619 (1928).

2. H. Bethe, Handbuch der Physik (Springer Verlag, Berlin, 1933), vol. 24, pt. 2, p. 595.

3. P. Weiss, J. Phys. 6, 661 (1907).

4. F. Bitter, Phys. Rev. 38, 1903 (1935).

5. C. G. Shull and J. S. Smart, Phys. Rev. 76, 1256 (1949).

6. A. Arrott, S. A. Werner, and H. Kendrick, Phys. Rev. Letters 16, 1022 (1965).

7. R. J. Weiss and K. J. Tauer, J. Phys. Chem. Solids 4, 135 (1958).

8. M. K. Wilkinson and C. G. Shull, Phys. Rev. 103, 516 (1956).

9. C. Kittel, Introduction to Solid State Physics, 2nd ed. (John Wiley and Sons, Inc., New York, 1956), p. 407.

10. S. C. Abrahams, J. Phys. Chem. Solids 24, 589 (1963).

11. C. G. Shull and M. K. Wilkinson, Rev. Mod. Phys. 25, 100 (1953).

12. T. H. Geballe, Rev. Mod. Phys. 36, 134 (1964).

13. B. T. Matthias, IBM J. Res. Develop. 6, 250 (1962).

14. W. C. Koehler, J. Appl. Phys. 36, 1078 (1965).

15. J. W. Cable, R. M. Moon, W. C. Koehler, and E. O. Wollan, Phys. Rev. Letters 12, 553 (1964).

16. K. A. Gschneidner, Jr., Rare Earth Alloys, (D. Van Nostrand Co. Inc., Princeton, New Jersey, 1961), p. 13.

17. G. Will, R. Nathans, and H. A. Alperin, J. Appl. Phys. 35, 1045 (1964).

18. W. C. Thoburn, S. Legvold, and F. H. Spedding, Phys. Rev. 112, 56 (1958).

19. S. Legvold, Rare Earth Research, ed. by E. V. Kleber, (The Macmillan Company, New York, 1961), p. 142.

20. F. J. Darnell, Phys. Rev. 130, 1825 (1963); F. J. Darnell, Phys. Rev. 132, 1098 (1963).

21. R. M. Bozorth and T. Wakiyama, J. Phys. Soc. Japan 17, 1669 (1962).

22. F. Barson, S. Legvold, and F. H. Spedding, Phys. Rev. 105, 418 (1957).

23. A. E. Clark, B. F. Savage, and R. Bozorth, Phys. Rev. 138, A216 (1965).

24. R. R. Birss, Proc. Roy. Soc. (London) A255, 398 (1960).

25. M. Griffel, R. E. Skochdopole, and F. H. Spedding, Phys. Rev. 93, 657 (1954).

26. M. Griffel, R. E. Skochdopole, and F. H. Spedding, J. Chem. Phys. 25, 75 (1956).

27. L. D. Jennings, R. M. Stanton, and F. H. Spedding, J. Chem. Phys. 27, 909 (1957).

28. A. H. Daane, The Rare Earths, ed. by F. H. Spedding and A. H. Daane (John Wiley and Sons, Inc., New York, 1961), p. 177.

29. P. C. Souers and G. Jura, Sci. 145, 575 (1964).

30. T. Mitsui and C, T. Tomizuka, Phys. Rev. 137, A564 (1965).

31. H. V. Malmstadt, C. G. Enke, and E. C. Toren, Electronics for Scientists (W. A. Benjamin, Inc., New York, 1963), p. 356.

32. G. Urbain, P. Weiss, and F. Trombe, Compt. rend. 200, 2132 (1935).

33. H. E. Nigh, S. Legvold, and F. H. Spedding, Phys. Rev. 132, 1092 (1963).

34. F. J. Darnell and W. H. Cloud, J. Appl. Phys. 35, 935 (1964).

35. L. Patrick, Phys. Rev. 93, 384 (1954).

36. D. Bloch and R. Pauthenet, Compt. rend. 254, 1222 (1962).

37. L. B. Robinson, F. Milstein, and A. Jayaraman, Phys. Rev. 134, A 187 (1964).

38. D. B. McWhan and A. L. Stevens, Phys. Rev. 139, A 682 (1965).

39. A. Jayaraman and R. C. Sherwood, Phys. Rev. Letters 12, 22 (1964).

40. R. M. Bozorth, Ferromagnetism (D. Van Nostrand Company, Inc., Princeton, New Jersey, 1951). p. 595.

41. W. D. Corner and F. Hutchinson, Proc. Phys. Soc. (London) 75, 781 (1960).

42. P. W. Montgomery, H. Stromberg, G. H. Jura, and G. Jura, High Pressure Measurement, ed. by A. A. Giardini and E. C. Lloyd (Butterworths, Washington, D.C., 1963), p. 1.

43. W. Stark and G. Jura, Lawrence Radiation Laboratory Report UCRL-11592, July, 1964.

44. R. M. Bozorth and T. Wakiyama, J. Phys. Soc. Japan 18, 97 (1963).

45. W. E. Coleman and A. S. Pavlovic, Phys. Rev. 135, A 426 (1964).

46. R. M. Bozorth, Ferromagnetism (D. Van Nostrand Company, Inc., Princeton, New Jersey, 1951), p. 725.

47. W. Klemm and H. Bommer, Z. anorg. u. allgem. Chem. 231, 138 (1937).

48. F. H. Spedding, S. Legvold, A. H. Daane, and L. D. Jennings, Progress in Low Temperature Physics, ed. by C. J. Gorter (North Holland Publishing Company, Amsterdam, 1957), vol. II, p. 368.

49. D. E. Hegland, S. Legvold, and F. H. Spedding, Phys. Rev. 131, 158 (1963).

50. W. C. Koehler, H. R. Child, E. O. Wollan, and J. W. Cable, J. Appl. Phys. 34, 1335 (1963).

51. C. E. Monfort, III, and C. A. Swenson, J. Phys. Chem. Solids 26, 623 (1965).

52. J. J. Rhyne and S. Legvold, Phys. Rev. 138, A507 (1965).

53. A. J. Freeman and R. E. Watson, Phys. Rev. 124, 1439 (1961).

54. P. W. Anderson, Magnetism, ed. by G. T. Rado and H. Suhl (Academic Press, New York, 1963), vol. I, p. 32.

55. R. J. Elliott, Magnetism, ed. by G. T. Rado and H. Suhl (Academic Press, New York, 1965), vol. IIA, p. 385.

56. M. A. Ruderman and C. Kittel, Phys. Rev. 96, 99 (1954).

57. S. H. Liu, Phys. Rev. 127, 1889 (1962).

58. P. W. Bridgman, Proc. Am. Acad. Arts Sci. 82, 83 (1953).

59. P. W. Bridgman, Proc. Am. Acad. Arts Sci. 83, 1 (1954).

60. H. Frauenfelder, The Mössbauer Effect (W. A. Benjamin, Inc., New York, 1962).

61. M. Nicol and G. Jura, Science 141, 1035 (1963).

62. D. N. Pipkorn, C. K. Edge, P. Debrunner, G. DePasquali, H. G. Drickamer, and H. Frauenfelder, Phys. Rev. 135, A1604 (1964).

63. L. Kaufman, Solids Under Pressure, ed. by W. Paul and D. M. Warschauer (McGraw-Hill Book Company, Inc., New York, 1963), p. 317.

64. M. Nicol, The Effect of Pressure on the Mössbauer Spectrum of Fe^{57} in Iron Metal (Ph.D. Thesis), UCRL-10785, May, 1963.

65. J. G. Dash, R. D. Taylor, D. E. Nagle, P. P. Craig, and W. M. Wisscher, Phys. Rev. 122, 1116 (1961).

66. R. V. Hanks, Phys. Rev. 124, 1319 (1961).

67. P. W. Bridgman, Proc. Am. Acad. Arts Sci. 74, 425 (1942).

68. A. Zeitlin and J. Brayman, High Pressure Measurement, ed. by. A. A. Giardini and E. C. Lloyd (Butterworths, Washington, D. C., 1963), p. 301.

69. D. McWhan, P. W. Montgomery, H.D. Stromberg, and G. Jura, J. Phys. Chem. 67, 2308 (1963).

FIGURE CAPTIONS

Fig. 1   A schematic diagram of Bridgman anvils. For the magnetic
         studies the anvils were made from Discalloy stainless steel
         and Kennametal·601 tungsten carbide. Also pictured is the
         normal procedure for making electrical resistance measurements.

Fig. 2   A horizontal cross-sectional view of the original apparatus
         for making magnetic measurements. A Bridgman anvil with two
         search coils in place is shown between the iron core electro-
         magnets. The pole tip extensions mentioned in the text are
         shown by the dashed lines.

Fig. 3   A schematic diagram of the second device for magnetic measure-
         ments. The iron frame with sample and dummy sides is shown
         with the field and signal coils in place.

Fig. 4   Isobaric magnetization-temperature curves for gadolinium.
         The pressure for each curve and the Curie point at one atmosphere
         are listed on the graph.

Fig. 5   The Curie temperature of Gd as a function of pressure. The
         line is a least squares linear fit of the experimental points.

Fig. 6   Isobaric magnetization-temperature curves of terbium. The
         pressure for each curve and the "Curie" and Néel points at
         one atmosphere are listed on the graph.

Fig. 7   Magnetization curves of Tb. The filled circles represent the
         magnetization-temperature behavior of freshly annealed Tb.
         The other curves represent the magnetization-temperature
         behavior at one atmosphere of Tb compressed to the pressures
         listed and then decompressed.

FIGURE CAPTIONS

Fig.8-11: Note the changes of scale on spectra taken with samples
placed inside or outside the anvils.

Fig. 8   Mössbauer spectrum of Fe^{57} in stainless steel 304 measured
relative to a stainless steel absorber. This spectrum was
taken at 1 atmosphere pressure and room temperature with
the sample placed outside the anvils.

Fig.9a   The top spectrum is the same as Fig. 8 but the sample is
placed in the anvils.

Fig.9b   The bottom curve is the Mössbauer spectrum of Fe^{57} in
stainless steel 304 measured relative to a stainless steel
absorber. This spectrum was taken at 1 atmosphere and room
temperature after compression to 130 kbars. The sample was
placed in the anvils.

Fig.10   This spectrum is the same as Fig. 9b but the sample was
placed outside the anvils.

Fig.11   The Mössbauer spectrum of Fe^{57} in stainless steel measured
relative to a stainless steel absorber. This spectrum was
taken at 60 kbars pressure and room temperature.

FIGURE CAPTIONS

Fig. 12   Schematic diagram of electrical resistance sample.

Fig. 13   Resistance-pressure behavior of Bi at 301°K.

Fig. 14   Deviation of experimental resistance points from an assumed

quadratic curve for the resistance from 32 to 85 kbars.

The results of three independent determinations are shown.

Three points in which the deviation was greater than 0.25%

are not shown.   There is no indication of any transitions

in the regions at 45 and 60 kbars.